Journal of Molecular Spectroscopy 258 (2009) 20–25

Contents lists available at ScienceDirect

Journal of Molecular Spectroscopy

journal homepage: www.elsevier.com/locate/jms

Fourier transform infrared emission spectroscopy of new systems of NiS

R.S. Ram [a,*], S. Yu [b], I. Gordon [c], P.F. Bernath [a,d,e]

[a] Department of Chemistry, University of Arizona, Tucson, AZ 85721, USA
[b] California Institute of Technology, Jet Propulsion Laboratory, Pasadena, CA 91109, USA
[c] Harvard-Smithsonian Center for Astrophysics, Cambridge, MA 02138, USA
[d] Department of Chemistry, University of Waterloo, Waterloo, Ont., Canada N2L 3G1
[e] Department of Chemistry, University of York, Heslington, York YO10 5DD, UK

ARTICLE INFO

Article history:
Received 9 July 2009
In revised form 21 August 2009
Available online 27 August 2009

Keywords:
Fourier transform emission spectroscopy
Near infrared spectroscopy
Rotational analysis
Transition metal sulfides

ABSTRACT

The emission spectrum of NiS has been investigated in the near infrared in the 2000–7500 cm^{-1} region using a Fourier transform spectrometer. New bands observed in the 3000–5000 cm^{-1} region have been assigned to a $^3\Pi_i$–$X^3\Sigma^-$ transition analogous to the transition of NiO observed in the near infrared [R.S. Ram and P.F. Bernath, J. Mol. Spectrosc. 155 (1992) 315–325]. The 0–0 band of NiS consists of $^3\Pi_{0+}$–$X^3\Sigma_1^-$ (4399 cm^{-1}), $^3\Pi_{0-}$–$X^3\Sigma^-$ (4257 cm^{-1}), $^3\Pi_1$–$X^3\Sigma_{0+}^-$ (3938 cm^{-1}), and $^3\Pi_2$–$X^3\Sigma_1^-$ (3325 cm^{-1}) sub-bands. To higher wavenumbers, another [$\Omega = 1$] - $X^3\Sigma_{0+}^-$ transition has been observed with a 0–0 *R* head near 5887 cm^{-1}. This transition has been assigned as $^1\Pi$–$X^3\Sigma_{0+}^-$, although a $^3\Pi_1$–$X^3\Sigma_{0+}^-$ assignment is also possible. Several vibrational bands belonging to different sub-bands were rotationally analyzed and spectroscopic constants evaluated. Our spectroscopic constants for the ground state agree well with the values reported in the microwave study by Yamamoto et al. [T. Yamamoto, N. Tanimoto, T. Okabayashi, Phys. Chem. Chem. Phys. 9 (2007) 3744–3748].

1. Introduction

In recent years, there has been considerable interest in spectroscopic studies of transition metal containing species because of their importance in chemistry, astrophysics, surface science and ab initio calculations. These compounds are widely used as catalysts in various chemical processes. The metal-oxygen and metal-sulfide bonds are of interest in explaining the bulk metal properties, since oxygen and sulfur atoms on the transition metal surface play an important role in these processes. The desulfurization catalysts (Ni–Mo), for example, are used in chemical processes intended to produce the sulfur-free fuel. The 3d transition metal-containing molecules have unique properties due to their d-electrons and the presence of many unpaired d-electrons increases the complexity of spectra due to spin–orbit interactions. Theoretical calculations on these molecules often fail to predict the correct spectroscopic properties and energy ordering of electronic states. The spectroscopic studies of these molecules, therefore, have become important to gain insight into chemical bonding in simple metal systems [1]. Because of the high cosmic abundance of transition metal elements in stars, transition metal-containing molecules are also of astrophysical importance [2,3]. In particular, transition metal sulfides such as TiS and ZrS are prominent in the near infrared spectra of S-type stars [4] and NiS might also be present.

Among Ni containing molecules, NiH [5–9], NiO [10–15], NiF [16–20] and NiCl [21–24] have been relatively well studied in the past few decades. For NiO, for example, the ground state is well characterized by microwave spectroscopy [10] and some low-lying excited electronic states are known from high resolution studies [11,12] and theoretical calculations [13–15]. For NiS on the other hand, more limited spectroscopic data are available to date. There are several theoretical studies on the spectroscopic properties of low-lying electronic states [15,25–27], all of which predict a $X^3\Sigma^-$ ground state. These studies suggest that the bonding and electronic structure of NiS is very similar to that of NiO, and the separations between the very low-lying excited states of the two molecules are also very similar (within 400 cm^{-1}). The close similarity between transition metal sulfide and oxide molecules in general provides a useful guide for the analysis of the spectra of sulfides.

An experimental observation of NiS has been reported by Zheng et al. [28] in the 495–555 nm regions. The NiS bands were produced by the reaction of sputtered Ni atoms with CS_2 in a free jet expansion and spectra were recorded by laser-induced fluorescence (LIF). The observed bands were assigned to a $[17.4]^3\Sigma^-$–$X^3\Sigma^-$ transition. They reported the first spectroscopic constants for the electronic states of NiS by rotational analysis of several

* Corresponding author. Address: Department of Chemistry, University of Arizona, Room 133, Old Chemistry Building, 1306 East University Boulevard, Tucson, AZ 85721-0041, USA. Fax: +1 520 621 8407.
E-mail address: rram@u.arizona.edu (R.S. Ram).

0022-2852/$ - see front matter © 2009 Elsevier Inc. All rights reserved.
doi:10.1016/j.jms.2009.08.013

bands, all having $v'' = 0$ of the $X^3\Sigma^-_{0+}$ state as their common lower state. In a more recent study of NiS, Yamamoto et al. [29] observed pure rotation spectra involving the $\Omega'' = 0^+$ and 1 spin components of the $X^3\Sigma^-$ state, and provided very accurate rotational and spin splitting constants for the $v'' = 0$ and 1 vibrational levels. These authors estimated the ground state vibrational constant using the Kratzer relation and also estimated the location of some low-lying excited states based on the interaction of these states with the ground state [30]. A comparison of available results for NiS shows that the ground state rotational constants and bond lengths obtained by Zheng at al. [28] in the LIF study differ considerably from the microwave values of Yamamoto et al. [29], as well as theoretical values available in literature [15,25–27].

In the present work we report on the observation of new NiS bands in the near infrared region (2500–7500 cm^{-1}). Most of these bands have been assigned to a $^3\Pi_i$–$X^3\Sigma^-$ transition with 0–0 bands of the $^3\Pi_{0+}$–$X^3\Sigma^-_1$, $^3\Pi_{0-}$–$X^3\Sigma^-_1$, $^3\Pi_1$–$X^3\Sigma^-_{0+}$, and $^3\Pi_2$–$X^3\Sigma^-_1$, 0–0 sub-bands located near 4399, 4257, 3938 and 3325 cm^{-1}, respectively. To the higher wavenumbers, a 0–0 band observed with an *R* head near 5887 cm^{-1} has been identified as a $[\Omega = 1]$–$X^3\Sigma^-_{0+}$ transition which has be assigned as a $[5.8]^1\Pi$–$X^3\Sigma^-_{0+}$ transition. A $^3\Pi_1$–$X^3\Sigma^-$ assignment is also possible for this transition. A number of bands involving $v'' = 0$, 1, and 2 and $v' = 0$, 1 vibrational levels of the ground and excited states have been observed and rotationally analyzed providing first spectroscopic data on the low-lying $A^3\Pi_i$ and $[5.8]^1\Pi$ excited states of NiS. The observation of the $A^3\Pi_i$–$X^3\Sigma^-$ transition of NiS is consistent with a similar transition of NiO in the near infrared region [11].

2. Experimental

The near infrared spectra of NiS were produced by the reaction of nickel atoms with about 30 mTorr of CS_2 in the presence of ~150 Torr of He in a high temperature carbon tube furnace (King furnace). The furnace was operated at a temperature of about 2200 °C. The emission from the furnace was focused on to the entrance aperture of a Bruker IFS 120 HR Fourier transform spectrometer using a CaF_2 lens and the spectra were recorded in the 2000–7500 cm^{-1} region using InSb detectors at a resolution of 0.04 cm^{-1}. About 100 scans were co-added in about one hour of integration.

The new emission bands were readily attributed to NiS based on their vibrational intervals and rotational line spacing. The spectral line positions were measured using a data reduction program called WSPECTRA written by M. Carleer of the Université Libre de Bruxelles. The peak positions were determined by fitting a Voigt line shape function to each experimental feature. The furnace spectrum also contained the vibration–rotation bands of HCl, HF and CO as impurities in addition to the NiS bands and some Ni atomic lines. We have used the HF line positions [31] to calibrate our spectra. The molecular lines appear with approximate widths of ~0.045 cm^{-1} and a maximum signal-to-noise ratio of about 13:1. The line positions are expected to be accurate to ±0.007 cm^{-1}. However, there is considerable blending of lines due to the overlap of rotational structure of different sub-bands of NiS as well as the much stronger vibration–rotation lines of HF and HCl and CO, so the uncertainty in measurement is somewhat higher for blended and weaker lines.

3. Observation and analysis

A careful inspection of the spectrum indicates the presence of a number of NiS bands in the 2500–7500 cm^{-1} region. The bands observed in the 5000–7500 cm^{-1} region are much weaker in intensity than the lower wavenumber bands. An overview of spectrum in the 3500–5000 cm^{-1} region is provided in Fig. 1. The very strong emission features present in this spectrum are due to HCl, HF and CO vibration–rotation lines. Absorption lines appearing in between 3600–4000 cm^{-1} interval are due to H_2O while some of the very strong lower J HCl and HF lines also appear in absorption. The branches in different bands were picked out using a color Loomis–Wood program running on a PC computer. The carrier of these bands was established by rotational analysis of the strong bands. The observation of isotopic lines of the most abundant isotopologues also established the carrier. Ni has five naturally occurring isotopes, ^{58}Ni, ^{60}Ni, ^{61}Ni, ^{62}Ni and ^{65}Ni with approximate abundances of 68.3%, 26.1%, 1.1%, 3.6% and 0.9%, respectively. In addition to the most abundant ^{58}NiS isotopologue, the rotational lines of the minor ^{60}NiS are expected to be present with ~30% of the intensity of ^{58}NiS. As expected, we were able to identify the rotational lines of both ^{58}NiS and ^{60}NiS in several strong bands, although data for ^{60}NiS were limited to a few $\Delta v \neq 0$ bands. In this work we obtained the rotational analysis only for the most abundant ^{58}NiS isotopologue.

A rotational analysis of the observed bands provides evidence for the presence of two new transitions, $^3\Pi_i$–$X^3\Sigma^-$ and $[\Omega = 1]$–$X^3\Sigma^-_{0+}$ in the near infrared with details provided in the following sections.

3.1. The $A^3\Pi_i$–$X^3\Sigma^-$ transition

The bands belonging to the $A^3\Pi_i$–$X^3\Sigma^-$ transition are located in the 2500–5000 cm^{-1} interval. This transition is analogous to the $A^3\Pi_i$–$X^3\Sigma^-$ transition of NiO with $T_{00} = 4337.6$ cm^{-1} [11] and is observed with $T_{00} = 3865$ cm^{-1}. The $A^3\Pi_i$ state of NiS is expected to obey Hund's case (a) coupling as in the case for NiO [11]. Each vibrational band should consist of $^3\Pi_{0\pm}$–$X^3\Sigma^-_1$, $^3\Pi_1$–$X^3\Sigma^-_{0+}$ and $^3\Pi_2$–$X^3\Sigma^-_1$ sub-bands. The strongest NiS band is located near 3938 cm^{-1} and is assigned as the 0–0 band of the $^3\Pi_1$–$X^3\Sigma^-_{0+}$ sub-band. Some other vibrational bands located at 3435, 3398 and 4398 cm^{-1} have been assigned as the 0–1, 1–2 and 1–0 bands of this sub-band, respectively. The rotational structure of each band of this sub-band consists of a single *P*, single *Q* and a single *R* branch. A portion of the 0–0 band of this sub-band is provided in Fig. 2. We have observed rotational lines up to $J = 79$, 113 and 78, respectively, in the *R*, *Q* and *P* branches.

On the higher wavenumber side, two bands located 4257 and 4399 cm^{-1} have been assigned as the $^3\Pi_{0-}$–$X^3\Sigma^-_1$, 0–0 and $^3\Pi_{0+}$–$X^3\Sigma^-_1$, 0–0 bands. The 4257 cm^{-1} band is overlapped by strong

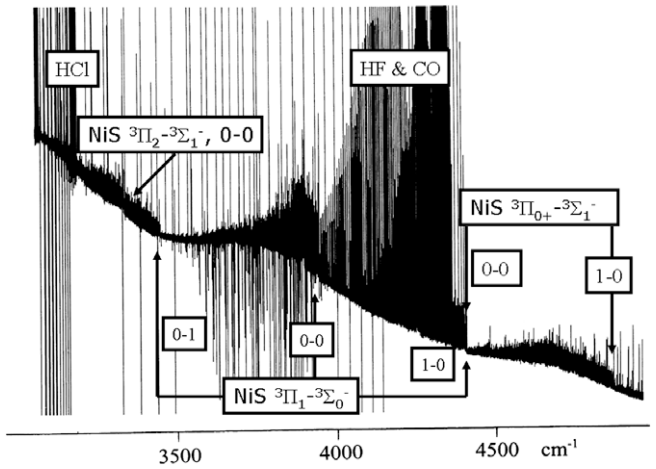

Fig. 1. A compressed portion of the spectrum of NiS in the 3000–5000 cm^{-1} region, marking the band heads of the $A^3\Pi_i$–$X^3\Sigma^-$ transition. The strong lines in the spectrum are due to the vibration–rotation bands of HCl, HF and CO molecules.

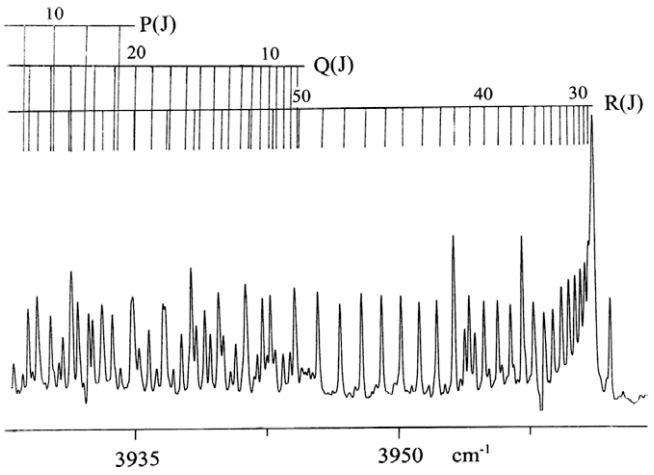

Fig. 2. A portion of the 0–0 band of the $A^3\Pi_1$–$X^3\Sigma^-_{0+}$ sub-band of NiS near the *R* head, marking some low *J* lines in the *R*, *Q* and *P* branches.

HF lines and has not been marked in Fig. 1. The $^3\Pi_{0+}$–$X^3\Sigma^-_1$, 0–0 band at 4399 cm^{-1} is overlapped with the 1–0 band of the $^3\Pi_1$–$X^3\Sigma^-_{0+}$ sub-band located in the same region. The rotational lines of this band were picked out easily using our Loomis–Wood program, in spite of overlapping. Another band observed at 4865 cm^{-1} has been assigned as the 1–0 band of the $^3\Pi_{0+}$–$X^3\Sigma^-_1$ sub-band. The corresponding 1–0 band of the $^3\Pi_{0-}$–$X^3\Sigma^-_1$ sub-band could not be assigned due to severe overlapping. The 0–1 band and higher vibrational bands of these two sub-bands were also not identified due to overlapping or weak intensity. Each band of these sub-bands consists of a single *P*, single *Q* and a single *R* branch as expected. A portion of the 0–0 band of the $^3\Pi_{0+}$–$X^3\Sigma^-_1$ sub-band near the band head has been provided in Fig. 3, in which some low *J* lines of the three branches have been marked. Rotational lines up to *R*(81), *Q*(131) and *P*(104) were observed. Another band located near 3325 cm^{-1} has been identified as the 0–0 band of the $^3\Pi_2$–$X^3\Sigma^-_1$ sub-band. As expected, this band consists of 2*R*, 2*Q* and 2*P* branches. No other vibrational bands associated with this sub-band have been identified in our spectra. No perturbations were detected in any of the observed bands.

3.2. The [5.8]$^1\Pi$–$X^3\Sigma^-_{0+}$ transition

A relatively weak band observed with *R* head at 5887 cm^{-1} has been identified as the 0–0 band of a $[\Omega = 1]$–$X^3\Sigma^-_{0+}$ transition. The upper state is most probably a $^1\Pi$ state, although a $^3\Pi_1$–$X^3\Sigma^-_1$ assignment cannot be completely ruled out. If this band is a $^3\Pi_1$–$X^3\Sigma^-_{0+}$ sub-band, we should have been able to find other associated sub-bands in the observed spectral range, but did not see any. Another band located to higher wavenumbers at 6315 cm^{-1} has been assigned as the 1–0 band. The corresponding 0–1 band is weaker than the other two bands but the *Q* lines were clearly identified in spite of very weak intensity. The lines of the 0–1 band of this sub-band were not included in the final fit because of the lack of sufficient data. A portion of the 0–0 band is provided in Fig. 4. This transition consists of a single *P*, a single *Q* and a single *R* branch as expected (Fig. 4). The $v' = 0$ vibrational level of this state is free from perturbations although there is evidence of weak interaction in the $v' = 1$ vibrational level for lines with $J < 45$ and $J > 98$. The rotational lines of the 0–0 and 1–0 bands were combined with the lines of the $A^3\Pi_i$–$X^3\Sigma^-$ transition in the final fit.

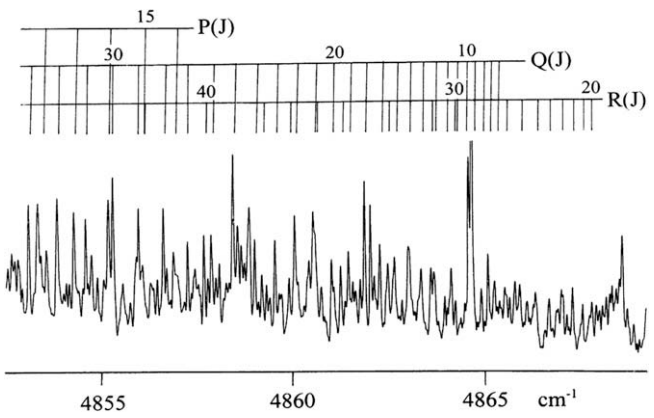

Fig. 3. A portion of the 1–0 band of the $A^3\Pi_{0+}$–$X^3\Sigma^-_1$ sub-band of NiS near the *R* head, marking some low *J* lines in the *R*, *Q* and *P* branches.

Rotational assignment in the different 0–0 and 0–1 bands were made by comparing the combination differences with the corresponding values for the $v'' = 0$ and 1 vibrational levels of the $X^3\Sigma^-_{0+}$ and $X^3\Sigma^-_1$ components of the $X^3\Sigma^-$ ground state calculated using the rotational constants from the microwave study by Yamamoto et al. [29]. The assignments in the other higher vibrational bands were made by matching the combination differences for common vibrational levels of the excited states. The spectroscopic constants for the different vibrational levels of the $^3\Pi$ and $^3\Sigma^-$ states were determined by fitting the observed line positions using the Hamiltonian matrix elements for these states provided elsewhere [32]. The energy levels of the $^1\Pi$ state are given by the following expression:

$$F_v(J) = T_v + B_v J(J+1) - D_v[J(J+1)]^2 \pm \frac{1}{2}\left\{q_v J(J+1) + q_{Dv}[J(J+1)]^2 + q_{Hv}[J(J+1)]^3\right\}$$

Because of some Hund's case (c) character in the $A^3\Pi$ state, a number of higher order parameters were needed in addition to T_0, A_0, B_0, D_0, p_0, o_0 and λ_0 for the $v = 0$ vibrational levels of the $A^3\Pi$ state. For the $v = 1$ vibrational level of this state several of these parameters were held fixed to the values from the $v = 0$ vibrational level because bands involving the $^3\Pi_{0-}$ and $^3\Pi_2$ components of the excited $v = 1$ vibrational level were not identified. The higher-lying state with $T_{00} = 5837$ cm^{-1} was treated as a $^1\Pi$ state in the final fit. For the ground $X^3\Sigma^-$ state, T_v, B_v, D_v, γ_v, γ_{Dv}, λ_v and λ_{Dv} were determined for the $v'' = 0$ vibrational level while for the v" $= 1$ vibrational level all of these constants except γ_{Dv} were determined in the final fit. For $v'' = 2$ vibrational level for which no bands involving the $X^3\Sigma^-_1$ spin component of the ground state were observed, the constants λ_v and λ_{Dv} were fixed to the values for the $v'' = 1$ vibrational level and the constants T_v, B_v, D_v and γ_v were determined. In the final fit weaker and blended lines were given lower weights. The microwave lines were also included with suitable weights in the final fit. The observed lines positions of both the transitions along with obs.-calc. residuals are available on ScienceDirect (www.sciencedirect.com) and as part of the Ohio State University Molecular Spectroscopy Archives (http://msa.lib.ohio-state.edu/jmsa_hp.htm). The spectroscopic constants obtained for the ground state are provided in Table 1 while those for the excited states are given in Table 2.

4. Discussion

There are several theoretical studies of NiO [13–15] and NiS [15,25–27] which have suggested that the spectroscopic properties of these two molecules should be very similar. Like NiO, the ground and the low-lying electronic states of NiS arise from the following configurations:

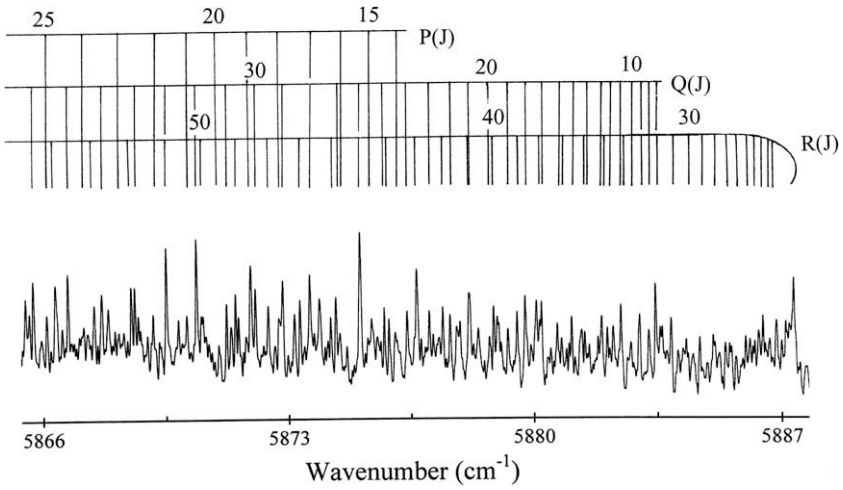

Fig. 4. A portion of the 0–0 band of the $[5.8]^1\Pi$–$X^3\Sigma^-_{0+}$ transition of NiS near the *R* head, marking some rotational lines in the *R*, *Q* and *P* branches.

$$(\delta)^4(\sigma)^2(\pi)^2 \rightarrow {}^3\Sigma^-, {}^1\Sigma^+, {}^1\Delta \quad \text{(i)}$$

$$(\delta)^4(\sigma)^1(\pi)^3 \rightarrow {}^3\Pi, {}^1\Pi \quad \text{(ii)}$$

$$(\delta)^4(\sigma)^1(\pi)^2(\sigma)^1 \rightarrow {}^3\Sigma^+ \quad \text{(iii)}$$

The $^3\Sigma^-$ state arising from configuration (i) is the ground state of NiS while the $A^3\Pi$ state observed in the present work arises from configuration (ii). These two configurations also result in the low-lying $^1\Sigma^+$, $^1\Delta$ and $^1\Pi$ states. In addition to the ground state, the spectroscopic properties of some low-lying excited states such as $^3\Pi$, $^3\Sigma^+$ and $^1\Sigma^+$ have been calculated by Bauschlicher [15] in his MRCI and MRCI + Q calculations. No predictions have been made for the spectroscopic properties of the $^1\Delta$ and $^1\Pi$ states in the theoretical calculations available so far. The observation of a $^3\Pi$ state at 3865 cm^{-1} is consistent with the theoretical values of 3610 and 4580 cm^{-1} in MRCI and MRCI + Q calculations. In the microwave study of NiS, Yamamoto et al. [29] have estimated the approximate location of the first excited $^3\Pi$ state assuming that the spin splitting constant γ in the ground $X^3\Sigma^-$ state arises entirely as a result of interaction of the ground state with the $^3\Pi$ excited state. With this approximation, the values of *B* and γ from the microwave study provided the $E_{3\Pi}$–$E_{3\Sigma+}$ separation of 3800 cm^{-1} which is in very good agreement with our experimental value of T_{00} = 3865 cm^{-1}. They also estimated the position of the higher-lying $^1\Sigma^+$ state at 8700 cm^{-1} through a second order interaction from this state. This state has been predicted at 12 350 and 14 040 cm^{-1} in the MRCI and MRCI + Q calculations by Bauschlicher [15]. No theoretical predictions are available for the other excited states of NiS. In this paper we have assigned the higher-lying Ω = 1 state observed with T_{00} = 5737 cm^{-1} as a $^1\Pi$ state arising from configuration (ii). As mentioned earlier, this state can equally well be assigned as the $^3\Pi_1$ component of another low-lying $^3\Pi$ state. The spectroscopic properties of the $^1\Pi$ state or other low-lying $^3\Pi$ states have not been predicted in the theoretical calculations.

The spectroscopic constants of Tables 1 and 2 were used to evaluate the equilibrium constants for the ground and excited states which are provided in Table 3. The observation of v = 0, 1 and 2 vibrational levels enables us to determine equilibrium constants, ω_e, $\omega_e x_e$, B_e, α_e and r_e, for the ground state. As only v = 0 and 1 vibrational levels were observed for the $A^3\Pi$ and $[5.8]^1\Pi$ states, only $\Delta G_{1/2}$ values could be obtained in addition to the equilibrium rotational constants. Our ground state vibrational constants of ω_e = 512.68(23) cm^{-1} and $\omega_e x_e$ = 3.610(92) cm^{-1} agree well with the values estimated using the microwave constants [ω_e = 507.227 cm^{-1} and $\omega_e x_e$ = 2.20341 cm^{-1}]. The equilibrium bond lengths of the low-lying electronic states

Table 1
Spectroscopic constants (cm^{-1}) for the $X^3\Sigma^-$ state of NiS.

Constants	v = 0	v = 1	v = 2
T_v	0.0	505.46(13)	1003.6998(19)
B_v	0.21185994(38)	0.21067732(35)	0.2093975(92)
$10^7 \times D_v$	1.49807(90)	1.5123(15)	1.4948(32)
γ_v	−0.107651(30)	−0.12133(70)	−0.11207(77)
$10^7 \times \gamma_{Dv}$	−4.835(86)	–	–
$10^{12} \times \gamma_{Hv}$	7.03(40)	–	–
λ_v	35.41570(85)	37.506(10)	37.506[a]
$10^5 \times \lambda_{Dv}$	5.425(43)	5.269(72)	5.269[a]

[a] Fixed values, see text for details.

are compared with the previous experimental and theoretical values in Table 4. One can notice from this table that the ground state constants of Zheng et al. [28] are far off from the present results, microwave results [28] and theoretical predictions available in the literature [15,25–27]. The bond length obtained by Zheng et al. [28] is 2.1195 Å, while a bond length of 1.962496(28) Å has been observed in the present work and 1.96248780(74) Å was obtained by Yamamoto et al. [29] in their study of pure rotational transitions. The values of 2.05 and 2.03 Å have, respectively, been calculated in the MRCI and MRCI + Q calculations of Bauschlicher [15] while a value of 1.97 Å has been predicted by and Bridgeman and Rothery [27] in their density functional calculations. It is interesting to compare the spectroscopic constants of NiS with those of NiO reported earlier [11]. The observation of the $A^3\Pi_i$ state 3865 cm^{-1} is consistent with the observation of the same state of NiO at 4337 cm^{-1}. The values of A_0 = −500.9925(27) cm^{-1} and o_0 = −68.974(21) cm^{-1} obtained for the $A^3\Pi_i$ state of NiS compare with the corresponding values of A_0 = −283.3713(16) cm^{-1} and o_0 = −29.7011(10) cm^{-1} for the $A^3\Pi_i$ state of NiO.

5. Conclusion

The emission spectrum of NiS has been observed in the near infrared using a Fourier transform spectrometer. The observed bands have been classified into two electronic transitions, $A^3\Pi_i$–$X^3\Sigma^-$ and $[5.8]^1\Pi$–$X^3\Sigma^-_{0+}$. The $A^3\Pi_i$ –$X^3\Sigma^-$, 0–0 band consists $^3\Pi_{0+}$–$X^3\Sigma^-_1$, $^3\Pi_{0-}$–$X^3\Sigma^-_1$, $^3\Pi_1$–$X^3\Sigma^-_{0+}$, and $^3\Pi_2$–$X^3\Sigma^-_1$ sub-bands located near 4399, 4257, 3938 and 3325 cm^{-1}, respectively. The higher wavenumber transition is much weaker in intensity than the lower wavenumber one and is assigned as a $[5.8]^1\Pi$–$X^3\Sigma^-_{0+}$

Table 2
Spectroscopic constants (cm^{-1}) for the $A^3\Pi_i$ and $[5.8]^1\Pi$ electronic states of NiS.

Constants	$A^3\Pi_i$		$[5.8]^1\Pi$	
	$v = 0$	$v = 1$	$v = 0$	$v = 1$
T_v	3864.5650(34)	4331.2618(43)	5837.5811(15)	6265.2501(18)
A_v	−500.9925(27)	−500.9925[a]	–	–
$10^3 \times A_{Dv}$	1.889(31)	1.889[a]	–	–
$10^8 \times A_{Hv}$	−2.2914(63)	−2.2914[a]	–	–
γ_v	0.3528(25)	0.37843(72)	–	–
$10^7 \times \gamma_{Dv}$	2.52(52)	–	–	–
B_v	0.20166282(52)	0.2009341(20)	0.19505595(85)	0.19386186(91)
$10^7 \times D_v$	1.4166(11)	1.5398(14)	1.6084(10)	1.5655(12)
$10^{13} \times H_v$	–	−2.434(50)	–	–
$10^4 \times q_v$	–	–	1.9337(57)	1.183(17)
$10^8 \times q_{Dv}$	2.155(31)	−0.6678(63)	–	1.096(56)
$10^{12} \times q_{Hv}$	−3.056(28)	–	–	−0.470(42)
p_v	−1.351(21)	0.7425(42)	–	
$10^5 \times p_{Dv}$	1.1964(60)	−1.513(17)	–	–
$10^{11} \times p_{Hv}$	4.30(55)	–	–	–
o_v	−68.974(21)	−68.974[a]	–	–
$10^4 \times o_{Dv}$	−4.0376(69)	−4.0376[a]	–	–
λ_v	−20.5911(17)	−16.1100(27)	–	–
$10^3 \times \lambda_{Dv}$	−0.190(46)	1.0267(69)	–	–

[a] Fixed values, see text for details.

Table 3
Equilibrium constants (cm^{-1}) for the low-lying electronic states of NiS.

Constants	$X^3\Sigma^-$	$A^3\Pi_i$	$[5.8]^1\Pi$
ω_e	512.68(23)	[466.6968(55)][a]	[427.6690(23)][a]
$\omega_e x_e$	3.610(92)	–	–
B_e	0.2124516(62)	0.2020272(12)	0.1956530(11)
α_e	0.0011831(54)	0.0007287(21)	0.0011941(13)
r_e (Å)	1.962496(28)	2.0124909(60)	2.0450108(58)

[a] Values in square brackets are $\Delta G_{1/2}$ values.

Table 4
Comparison of experimental and theoretical values of some spectroscopic constants of the low-lying electronic states of NiS.

Methods	T_{00} (cm^{-1})	r_e (Å)	ω_e (cm^{-1})
$X^3\Sigma^-$ State			
FTS [this work]	–	1.962496(28)	512.68(23)
MW [29]	–	1.962	507
LIF [28]	–	2.1195[a]	322[a]
MRCI [15]	–	2.05	490
MRCI + Q [15]	–	2.03	490
DFT [27]	–	1.97	513
$A^3\Pi_i$			
FTS [this work]	3864.5650(34)	2.0124909(60)	[466.6968(55)][b]
MW [29]	∼3800[c]	–	–
MRCI [15]	3610	2.15	390
MRCI + Q [15]	4580	2.11	370
$[5.8]^1\Pi$			
FTS [this work]	5837.5811(15)	2.0450108(58)	[427.6690(23)][b]
$^1\Sigma^+$			
MW [29]	8700[c]	–	–
MRCI [15]	12350	–	–
MRCI + Q [15]	14040	–	–
$^3\Sigma^+$			
MRCI [15]	16700	–	–
MRCI + Q [15]	18840	–	–

[a] The values from Ref. [28] do not agree with the values from other studies.
[b] $\Delta G_{1/2}$ value.
[c] Values estimated by Yamamoto et al. [29] from the interactions of the low-lying excited states with the ground state.

transition. The 0–0 and 1–0 bands of this transition were observed with *R* heads near 5887 and 6315 cm^{-1}.

Acknowledgments

The research described here was partially supported by funds from the NASA laboratory astrophysics program. Some support was also provided by the Natural Sciences and Engineering Research Council (NSERC) of Canada and the UK Engineering and Physical Sciences Research Council (EPSRC).

Appendix A. Supplementary data

Supplementary data associated with this article can be found, in the online version, at doi:10.1016/j.jms.2009.08.013. Supplementary data for this article are available on Science Direct (www.sciencedirect.com) and as part of the Ohio State University Molecular Spectroscopy Archives (http://library.osu.edu/sites/msa/jmsa_hp.htm).

References

[1] C.W. Bauschlicher Jr., S.P. Walch, S.R. Langhoff, Quantum chemistry: the challenge of transition metals and coordination chemistry, in: A. Veillard (Ed.), NATO ASI Ser. C, Reidel, Dordrecht, 1986.
[2] C. Jascheck, M. Jascheck, The Behavior of Chemical Elements in Stars, Cambridge Univ. Press, Cambridge, 1995.
[3] J.D. Kirkpatrick, I.N. Reid, J. Liebert, R.M. Cutri, B. Nelson, C. Beichman, C.C. Dahn, D.G. Monet, J.E. Gizis, M.F. Skrutskie, Astrophys. J. 519 (1999) 802–833.
[4] R.R. Joyce, K.H. Hinkle, L. Wallace, M. Dulick, D.L. Lambert, Astronom. J. 116 (1998) 2520–2529.
[5] R. Scullman, J.A. Gray, M. Li, R.W. Field, J. Mol. Spectrosc. 140 (1990) 126–140.
[6] S. Adakkai Kadavathu, R. Scullman, R.W. Field, J.A. Gray, M. Li, J. Mol. Spectrosc. 147 (1991) 448–470.
[7] T. Nelis, S.P. Beaton, K.M. Evenson, J.M. Brown, J. Mol. Spectrosc. 148 (1991) 462–478.
[8] L.C. O'Brien, J.J. O'Brien, Astrophys. J. 621 (2005) 554–556.
[9] P.F. Bernath, Transition metal monohydrides, in: M. Duncan (Ed.), Advances in Metal and Semiconductor Clusters, Elsevier, 2001.
[10] K. Namiki, S. Saito, Chem. Phys. Lett. 252 (1996) 343–347.
[11] R.S. Ram, P.F. Bernath, J. Mol. Spectrosc. 155 (1992) 315–325.
[12] E.J. Friedman-Hill, R.W. Field, J. Mol. Spectrosc. 155 (1992) 259–276.
[13] S.P. Walch, W.A. Goddard, J. Am. Chem. Soc. 100 (1978) 1338.
[14] C.W. Bauschlicher Jr., C.J. Nelin, P.S. Bagus, J. Chem. Phys. 82 (1985) 3265–3276.
[15] C.W. Bauschlicher Jr., Chem. Phys. 93 (1985) 399–404.
[16] C. Dufour, B. Pinchemel, J. Mol. Spectrosc. 173 (1995) 70–78.
[17] M. Tanimoto, T. Sakamaki, T. Okabayashi, J. Mol. Spectrosc. 207 (2001) 66–69.
[18] B. Pinchemel, T. Hirao, P.F. Bernath, J. Mol. Spectrosc. 215 (2002) 262–268.
[19] Y. Krouti, T. Hirao, C. Dufour, A. Boulezhar, B. Pinchemel, P.F. Bernath, J. Mol. Spectrosc. 214 (2002) 152–174.

[20] M. Benomier, A. van Groenendael, B. Pinchemel, T. Hirao, P.F. Bernath, J. Mol. Spectrosc. 233 (2005) 244–255.
[21] Y. Krouti, A. Poclet, T. Hirao, B. Pinchemel, P.F. Bernath, J. Mol. Spectrosc. 210 (2001) 41–50.
[22] L.C. O'Brien, K.M. Homann, T.L. Kellerman, J.J. O'Brien, J. Mol. Spectrosc. 211 (2002) 93–98.
[23] J.J. O'Brien, J.S. Miller, L.C. O'Brien, J. Mol. Spectrosc. 211 (2002) 248–253.
[24] S. Tumturk, L.C. O'Brien, J.J. O'Brien, J. Mol. Spectrosc. 225 (2004) 225–229.
[25] A.B. Anderson, S.Y. Hong, J.L. Samialek, J. Phys. Chem. 91 (1987) 4250–4254.
[26] C.W. Bauschlicher Jr., P. Maitre, Theor. Chem. Acta 90 (1995) 189–203.
[27] A.J. Bridgeman, J. Rothery, J. Chem. Soc. Dalton Trans. 118 (2000) 211–218.
[28] X.F. Zheng, T.T. Wang, J.R. Guo, C.X. Chen, Y. Chen, Chem. Phys. Lett. 394 (2004) 137–140.
[29] T. Yamamoto, N. Tanimoto, T. Okabayashi, Phys. Chem. Chem. Phys. 9 (2007) 3744–3748.
[30] W. Gordy, R.L. Cook, Microwave Molecular Spectra, 3rd ed., Wiley, New York, 1984.
[31] R.B. LeBlanc, J.B. White, P.F. Bernath, J. Mol. Spectrosc. 164 (1994) 575–579.
[32] C.R. Brazier, R.S. Ram, P.F. Bernath, J. Mol. Spectrosc. 120 (1986) 381–402.